3.4.6

Beam flattening system based on nonlinear optics for high-intensity spallation neutron source

Shin-ichiro Meigo, Motoki Ohi, Kiyomi Ikezaki and Atsushi Akutsu

J-PARC Center, Japan Atomic Energy Agency, Tokai, Ibaraki 319-1195, Japan

E-mail: meigo.shinichiro @jaea.go.jp

Hiroshi Fujimori

J-PARC Center, High Energy Accelerator Research Organization (KEK), Tsukuba, Ibaraki 305-0801, Japan

Abstract. The Japan Spallation Neutron Source of the Japanese Proton Accelerator Research Complex generates a high-power proton beam (up to 1 MW) for collision with a mercury target. With increasing beam power, the target damage becomes increasingly serious. For the high-power short-pulse spallation neutron source, the damage inflicted by the proton beam on the target vessel containing a liquid metal target such as mercury is proportional to the fourth power of the peak intensity of the proton beam. Reducing the peak current density at the target is vital for constant beam operation. To this end, we developed nonlinear beam optics based on octupole magnets. However, to obtain a completely flat beam distribution, higher-order magnets are required. We found that a significantly flat beam distribution can be obtained by reducing the magnetic field of the octupole magnet. Calculations indicate that, by introducing octupole magnets, the peak current density can be reduced by 30%.

1. Introduction

The Japan Proton Accelerator Research Complex (J-PARC) [1] (shown in Fig. 1) now includes a MW-class pulsed neutron source that was installed in the Materials and Life Science Experimental Facility (MLF) of the Japan Spallation Neutron Source (JSNS) [2] and the Muon Science Facility [3]. Since 2008, this source has produced a high-power proton beam of 300 kW. To produce a neutron source, a 3 GeV proton beam collides with a mercury target, and to produce a muon source, the 3 GeV proton beam collides with a 20-mm-thick carbon graphite target. To efficiently use the proton beam for particle production, both targets are aligned in a cascade scheme, with the graphite target placed 33 m upstream of the neutron target. For both sources, the 3 GeV proton beam is delivered from a rapid cycling synchrotron (RCS) to the targets by the 3NBT (3 GeV RCS to Neutron facility Beam Transport) [4-6]. Before injection into the RCS, the proton beam is accelerated up to 0.4 GeV by a LINAC. The beam is accumulated in two short bunches and accelerated up to 3 GeV in the RCS. The extracted 3 GeV proton beam, with a 150 ns bunch width and a spacing of 600 ns, is transferred to the muon production target and the spallation neutron source.
Recently, pitting damage became evident in the mercury target container [7], and the extent of the damage is proportional to the fourth power of the peak current density of the proton beam [8]. After

operating the beam at high power, significant pitting damage was observed at the spent mercury target vessel at JSNS and at the Spallation Neutron Source in Oak Ridge National Laboratory [9, 10]. Using linear optics (i.e., quadrupole magnets) for beam transport, the peak current density can be reduced by expanding the beam at the target. However, beam expansion increases heat in the vicinity of the target, where shielding and the neutron reflector are located. Therefore, the peak current density is limited by the heat induced in the vicinity of the target. At the JSNS, the minimum peak current density is expected to be 9 μA/cm^2, which gives a thermal energy density at the target of 14 J/cc/pulse [11]. Because the pitting damage goes as the fourth power of the peak density, scanning the beam with a deflecting magnetic field will not mitigate the pitting damage.
To reduce the peak current density while conserving the integrated beam current, the beam profile should be flat. To obtain a flat beam profile, beam rastering, which uses pulsed magnets to create a flat time-averaged profile at the target, is a possible method. However, rastering does not help mitigate pitting damage to the target vessel. For a uniformly shaped beam, pitting damage per pulse to the target vessel is given by D1 in the following equation:

$$D_1 = \int (C/S_1)^4 \, dt, \tag{1}$$

where S1, C, and t are the beam cross-sectional area at the target, the beam charge per pulse, and the irradiation time, respectively. For beam rastering, pitting damage is described by

$$D_2 = \int (C/S_2)^4 \, P \, dt, \tag{2}$$

where S_2 and P are the beam cross-sectional area for rastering and the beam-position probability, respectively. To obtain a flat time-averaged beam profile over S_1, P is given by

$$P = S_2/S_1. \tag{3}$$

Using Eq. (2), pitting damage for beam rastering can be described by

$$D_2 = \int (C/S_2)^4 \, S_2/S_1 \, dt = D_1 (S_1/S_2)^3. \tag{4}$$

With beam rastering, damage D_2 is proportional to the third power of the ratio of the total beam cross-sectional area to the beam cross-sectional area of each pulse. Therefore, beam rastering cannot sufficiently mitigate pitting damage at the mercury target vessel.
In this paper, we describe a system of nonlinear beam optics and discuss the side effects involved with such a system, such as misalignment of the beam at the target. To reduce the peak current density, we developed a beam-flattening system based on nonlinear beam optics.

2. Design of nonlinear beam optics

The 3 GeV proton beam extracted from the RCS is well described by a simple Gaussian [6]. With ordinary (i.e., linear) beam optics, the beam shape remains a Gaussian at all positions along the beam path. Using nonlinear optics, the beam particles located at the beam periphery are deflected toward the beam center, which flattens the beam distribution. To obtain a flat distribution in both the horizontal and vertical directions, two octupole magnets are required. These octupole magnets can be placed anywhere upstream of the target except where the phase advance between the magnets and the mercury target is an integer multiple of π. Because the targets have been irradiated by the proton beam for 5 years, the radiation dose around the targets is too high to place a magnet there. Therefore, the two octupole magnets (OCT1, OCT2) were placed upstream of the muon target, as shown in Fig. 2.

2.1. Octupole Magnetic Field

Starting with a beam that has a Gaussian distribution in transverse phase space, the multipole magnetic fields are given by [12]

$$K'_{2n} = \frac{(n-2)!}{(n/2-1)!}\frac{(-1)^{n/2}}{(2\varepsilon\beta)^{n/2-1}}\frac{1}{\beta\tan\varphi} \qquad (n = 4, 6, 8, \cdots) \tag{5}$$

to obtain a flat beam distribution at the target. In Eq. (5), K'_{2n} is the integrated strength of the 2n-pole multipole magnet, with the magnet assumed to be a thin lens for simplicity. The quantity ε is the root mean square (rms) of the transverse emittance (π mm mrad), β is the beta function (m) at the octupole magnet, and ϕ is the phase advance between the octupole magnet and the target. Using Eq. (5), the required octupole magnetic field is

$$K'_8 = (\varepsilon\beta^2\tan\varphi)^{-1}. \tag{6}$$

In Eq. (5), magnetic field orders greater than octupole are required to obtain a completely flat distribution. Without a dodecapole magnetic field in Eq. (5), the beam distribution is not flat but is peaked at the edge of the beam [12, 13]. Note that such edge peaks can be easily eliminated at low-energy accelerator facilities using a beam collimator. For a high-power, medium-energy accelerator facility such as the JSNS, the edge peak cannot be easily eliminated. The principle of beam flattening systems is to bend the beam from the edge of the beam toward the center using high-order magnetic fields. At the center of the target, the peak intensity of the beam does not change significantly upon using high-order magnetic fields. Bending the beam toward the center of the beam with high-order magnetic fields causes the beam intensity to increase in the tail part of the beam. Therefore, the intensity of the edge peak can be reduced by decreasing the strength of the high-order magnetic fields, although the edge shape blurs.

We now consider the case in which the beam has a uniform distribution in transverse phase space. For this, the octupole field required is [14]

$$K''_8 = \cos^3\varphi/12\varepsilon\beta^2\sin\varphi, \tag{7}$$

where K''_8 is the octupole field required to obtain a beam with uniform distribution in phase space. In Eq. (7), the distribution in real space cannot be completely flat but, by averaging Eqs. (6) and (7), is expected to evolve into a flat distribution with the edge peak suppressed:

$$K_8 = (K'_8 + K''_8)/2. \tag{8}$$

Using the octupole magnetic field K_8 given by Eq. (8), a flat beam distribution can be obtained, as shown in Fig. 3. Although the distribution shown in Fig. 3 is not completely flat and the edge is not sharper than that obtained by Eq. (5), the edge peak can still be well suppressed.

3. Beam Flattening System at JSNS

The beam optics for an entire beam transport line is shown in Fig. 4, which shows the beta and dispersion functions from the RCS to the mercury target. To achieve a flat beam distribution, the octupole field must be proportional to the inverse square of the beta functions described in Eqs. (2) and (3). Because of the high momentum of the present beam, a large octupole field is difficult to attain. To obtain a flat beam distribution with an octupole magnet having a realistic K, the beam width at the octupole magnet is expanded to a large β value. The physical aperture of the quadrupole magnets was fixed at 300 mm; therefore, we set the physical aperture of the octupole magnets to 300 mm. For linear beam optics, the admittance of the beam is designed to be 324 π mm mrad, which is given by the beam collimator placed at the RCS. A recent study of the RCS [15] shows that the transverse emittance will be reduced to as little as 250 π mm mrad. Therefore, the beam admittance at the octupole magnet must be 250 π mm mrad and β is set to 200 m at the octupole magnets.

3.1. Octupole magnets

Based on the optics design, the two pieces of the octupole magnet shown in Fig. 5 were fabricated. The design magnetic field gradient is 800 T/m^3 and the magnet has a bore diameter of 0.3 m and is 0.6 m long in the direction of the pole. We used a Hall probe to measure the magnetic field gradient and confirmed that the magnetic field was consistent with the design value. During actual beam operation, beam centering at the octupole is important. To center the beam, a beam position monitor (BPM) was installed in each magnet. The octupole magnets were installed in the beam transport system in the autumn of 2013. With the octupole magnets excited, the beam profile was measured in front of the mercury target.

4. Result and discussion

4.1. Calculation of beam profile

To calculate the beam profile at the neutron source, we used the DECAY-TURTLE [16] code revised by the Paul Scherrer Institute (PSI) [17]. With the modification implemented by the PSI, beam transport calculations include octupole magnetic fields and beam scattering from the carbon target.

4.2. Comparison with experimental results

Figure 6 shows preliminary results of the measured beam profile with (black) and without (cyan) excitation of the octupole magnets. These results for the beam profile were obtained by a multiwire profile monitor (MWPM) placed at the proton beam window, 1.8 m upstream of the mercury target. For simplicity, the muon production target was placed outside the beam. The results of the calculation with and without excitation of the octupole magnets are also shown in Fig. 6 (lines). The calculation results are consistent with the experiment results both with and without excitation of the octupole magnets. Figure 6 also compares the profile with the muon target and the octupole field. We observed that the calculated beam distribution is more Gaussian than the measured beam distribution, which might be due to an excessive prediction of the scattering effect in the calculation. By accounting for this phenomenon, the calculation should provide a conservative peak density.

4.3. Effect of misaligned magnets

In actual beam operation, a misaligned magnet causes beam divergence. A survey has shown that the floor of the beamline facility settled unevenly after an earthquake and the water table underlying the tunnel shifted; therefore, we cannot avoid beam divergence. In this section, we discuss the effect of misalignment on the beam profile based on the beam optics shown in Fig. 4. To simplify the calculation, the beam profile is calculated without beam scattering at the muon target.
To identify the alignment tolerance of the octupole magnet, the beam profile at the target is calculated with the beam position offset at the octupole magnet. Without shifting the beam at the octupole magnet, the beam distribution is flat. For a horizontal offset of 2 mm in the beam position at the octupole magnet, the beam shape has a peak at the beam edge where the intensity increases by approximately 8%, as shown in Fig. 7. At the mercury target, the peak at the edge causes greater damage than the peak at the center. The maximum increase in intensity at the edge is considered to be

approximately 4%. Therefore, the allowable beam shift at the octupole magnet is approximately 1 mm. To adjust the beam position at the octupole magnet, BPMs will be installed. By installing BPMs and additional steering magnets, the beam position can be statically centered at the octupole magnets. In each beam shot, a fluctuation in horizontal position occurs because of the instability of the kicker magnet at the RCS. However, the instability for each shot is less than 1 mm so that the edge peak does not cause difficulties.
To calculate the tilting tolerance of the octupole magnet, we considered the case of 0.5 mrad. We observed that the tilting error does not influence the beam shape. Because the precision of the angular position of the octupole magnet is less than 0.2 mrad, tilt misalignment is not a problem. Downstream of the octupole magnets, six pieces of the quadrupole magnets were positioned around the muon production target. To obtain the required accuracy for the position of the downstream magnets, beam profiles were calculated for the quadrupole magnets with the beam offset. We found that misalignment of the quadrupole magnets caused the beam position to oscillate because of betatron oscillation. Thus, misalignment of the quadrupole magnets does not influence the beam shape, and the flat beam distribution at the target is preserved. Because the beam position at the target can be adjusted easily using the steering magnets, misalignment of the quadrupole magnets downstream of the octupole magnets is not an issue for beam flattening.

4.4. Effect of beam scattering at muon production target

To minimize the peak density and obtain a flat beam distribution at the neutron production target, we studied the effect of beam scattering from the muon target. For the octupole magnets in use, the beam distribution in horizontal phase space, before it penetrates the carbon target (for muon production), is shown in Fig. 8. We observed that the octupole magnetic field generates an arm-shaped distribution in phase space. The beam particles in the arm region play an important role in beam flattening at the mercury target. Figure 9 shows the beam distribution after it passes the carbon target. The beam divergence, which is plotted on the vertical axis of Fig. 9, is widely spread by the scattering so that the beam distribution becomes similar to a Gaussian. To maintain a flat distribution, this increase in beam divergence due to scattering should be suppressed. Therefore, to obtain a flat distribution, the beam should be focused at the muon production target to increase the beam divergence at the target.

5. Conclusion

To reduce the peak current density of the beam at the target, we developed a beam transport system that uses nonlinear beam optics (i.e., octupole magnets). The results of calculations show that the beam can be flattened using optics with a large beta function at the octupole magnets and by ensuring an appropriate phase advance between the octupole magnets and the mercury target. Furthermore, we studied how magnet misalignment affects the beam profile. With the beam offset at the octupole magnet, the beam density becomes large at the target edge. The acceptable offset of the beam at the octupole magnet is approximately 1 mm, which is a feasible precision for the present beam operation. The results of simulations show that the alignment error of quadrupole magnets located downstream of the octupole magnets does not influence the shape of the beam at the target. To reduce a severe increase in the beam emittance because of the scattering from the muon production target, the beam is focused at the muon production target to obtain a large beam divergence. Calculations that consider beam scattering from the muon production target indicate that the peak current density can be reduced by approximately 30% from the peak density without the nonlinear beam optics.
Octupole magnets have already been installed in the proton transport line, and the calculated beam profile is consistent with the beam profile obtained with octupole magnets in place. Note that the

present nonlinear optics system represents the first attempt to install such a system in a MW-class hadron accelerator.

References

[1] The Joint Project Team of JAERI and KEK, JAERI-Tech 99-56, 1999.
[2] Y. Ikeda, Nucl. Instrum. Meth. A600, (2009) 1.
[3] Y. Miyake, et al., Physica B 404 (2009) 957.
[4] S. Meigo, et al., Nucl. Instrum. Meth. A562, (2006) 569.
[5] S. Sakamoto, et al., Nucl. Instrum. Meth. A562, (2006) 638.
[6] S. Meigo, et al., Nucl. Instrum. Meth. A600, (2009) 41.
[7] M. Futakawa, et al., J. Nucl. Sci. Technol. 40 (2004) 895.
[8] M. Futakawa, et al., J. Nucl. Mater. 343 (2005) 70.
[9] T. Naoe, et al., J. Nucl. Mater. 450 (2014) 123.
[10] D. A. McClintock, et al., J. Nucl. Mater., 431 (2012) 147.
[11] S. Meigo, et al., MOPEB066, IPAC10 (2010)
[12] Y. Yuri, et al., Phys Rev ST Accel. Beams 10, 10401 (2007).
[13] N. Tsoupas, et al., Nucl Sci. and Eng. 126 71 (1997).
[14] F. Meot and T. Aniel, Nucl. Instrum. Meth. A 379, 196 (1996).
[15] H. Hotchi, et al., THPPP080, IPAC12 (2012)
[16] K.L. Brown, Ch. Iselin and D.C. Carey: Decay Turtle, CERN 74-2 (1974)
[17] PSI Graphic Turtle Framework by U. Rohrer based on a CERN-SLAC-FERMILAB version

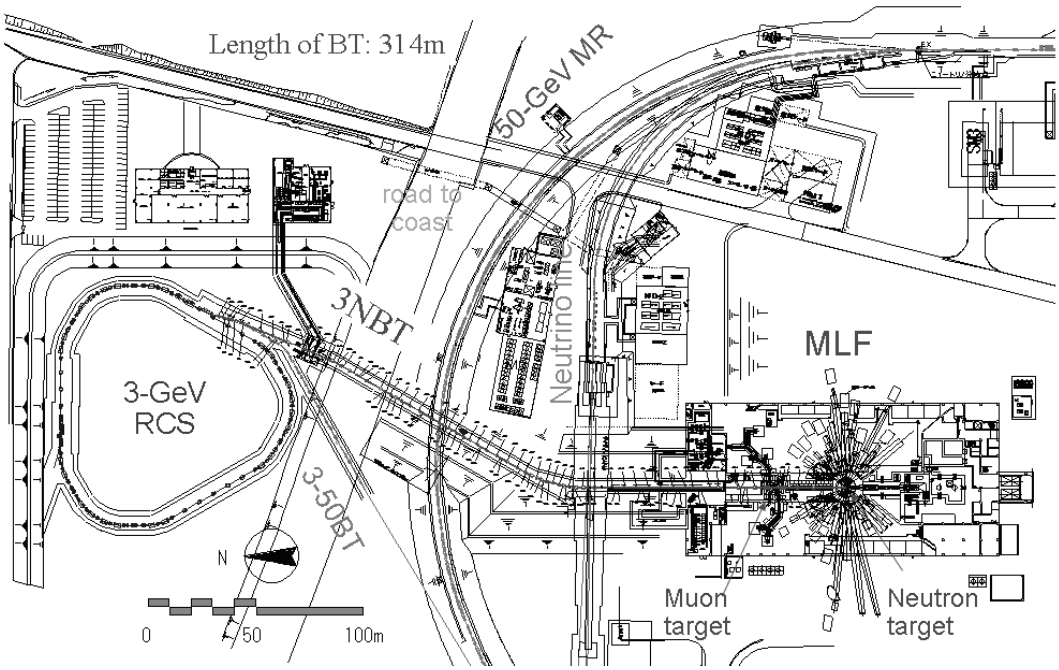

Figure 1: Plan of rapid cycling synchrotron (RCS) at the Materials and Life Science Experimental Facility at J-PARC.

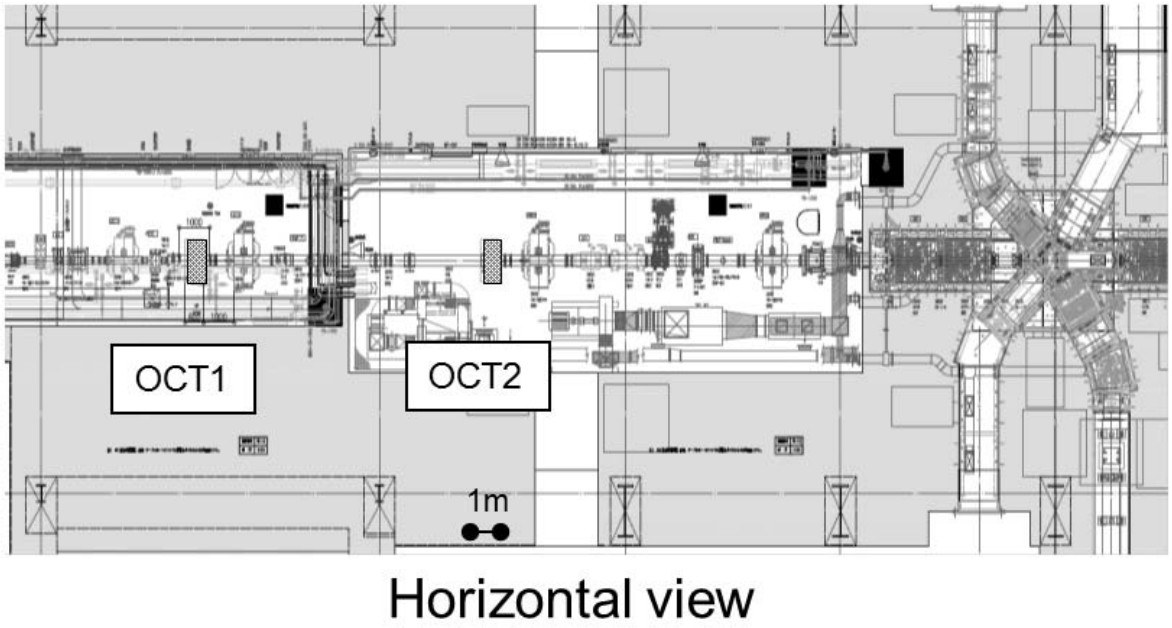

Figure 2: Plan of octupole magnets for beam expander system, which is to be placed upstream of muon production target

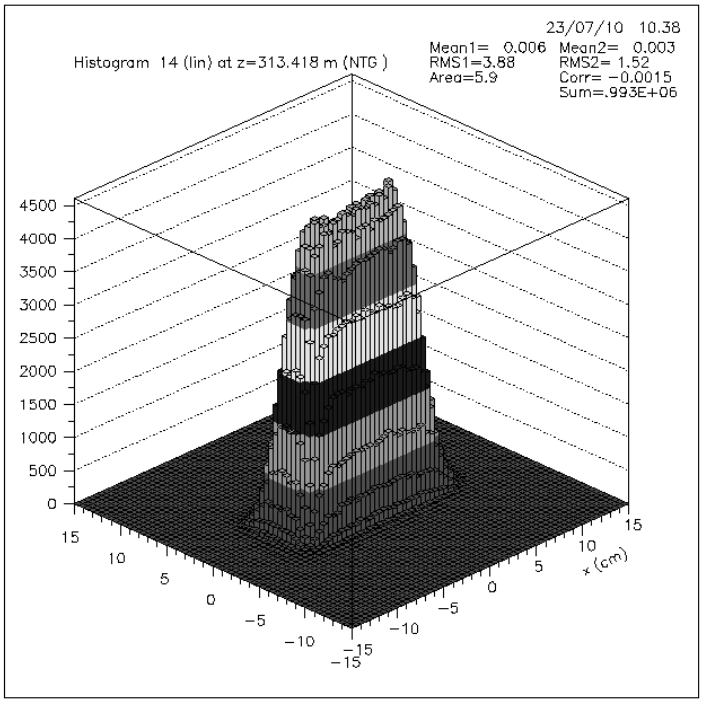

Figure 3: Flat beam distribution at the mercury target expanded by octupole magnets. Beam scattering from the muon production target is ignored.

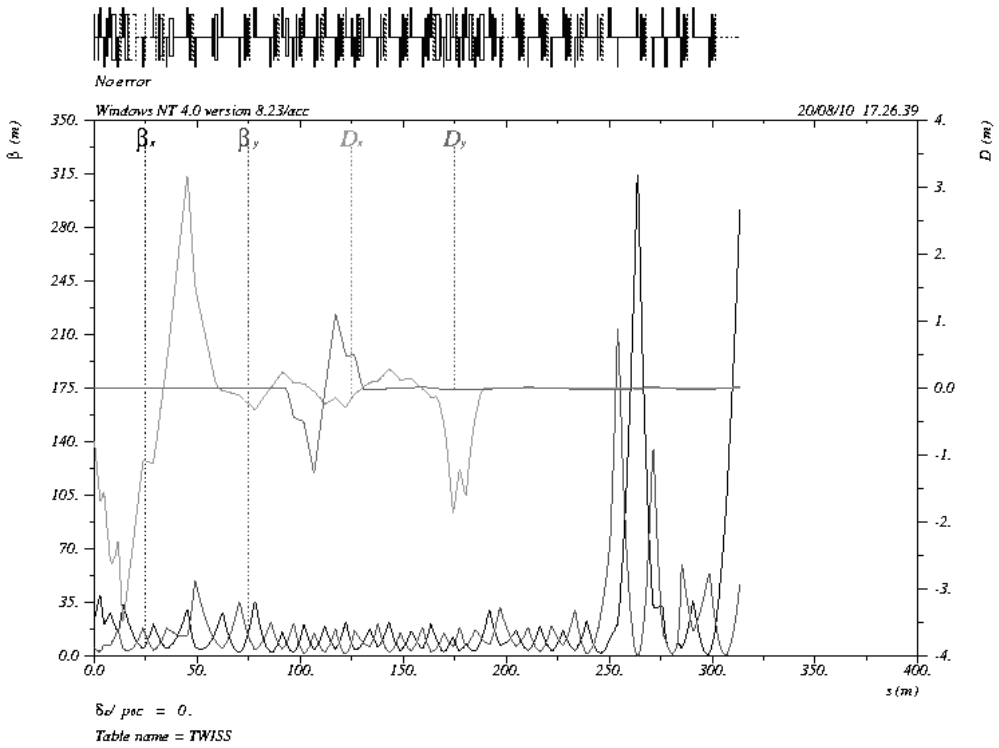

Figure 4: Beam optics and beta function for beam expander consisting of octupole magnets.

Figure 5: Fabricated octupole magnet with magnetic field gradient of 800 T/m^3.

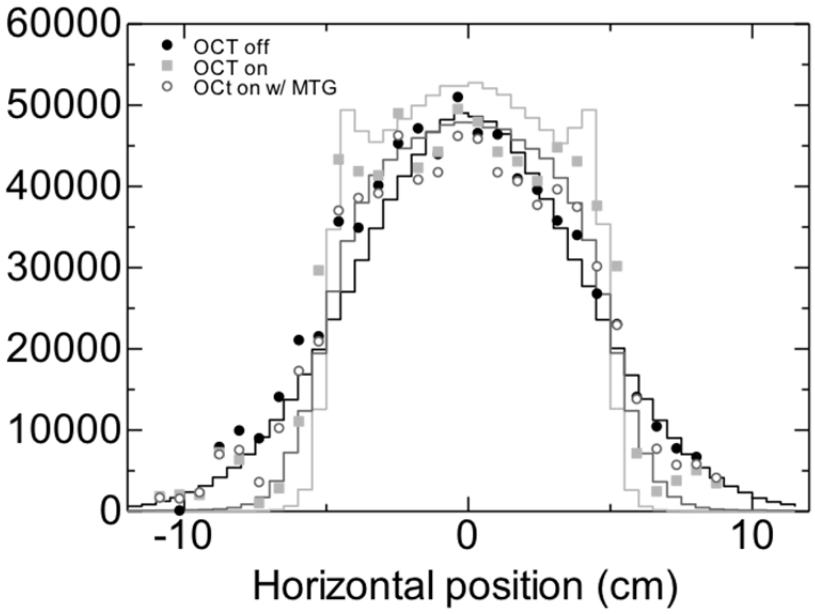

(a)

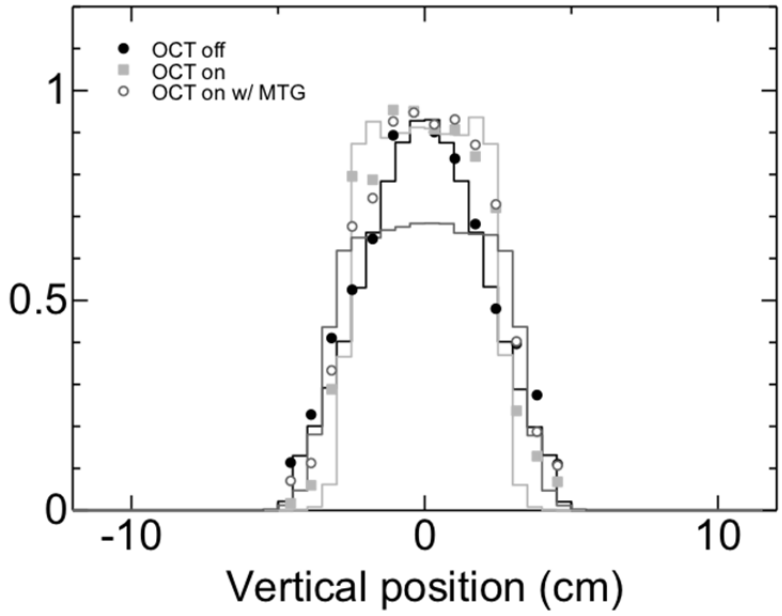

(b)

Figure 6: Beam profile in (a) horizontal and (b) vertical directions obtained by the MWPM (dots) compared with calculation by DECAY-TURTLE (lines) without octupole magnet excitation (black), with octupole magnet excitation (cyan), and with octupole magnet excitation and irradiation of muon production target (red).

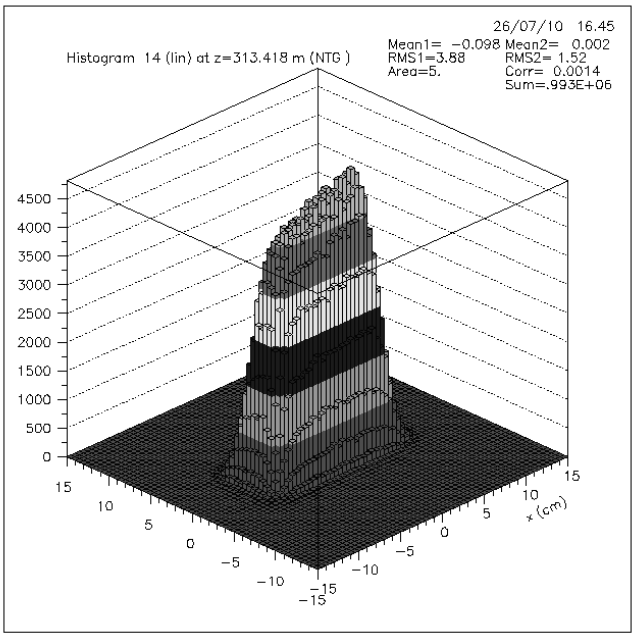

(a)

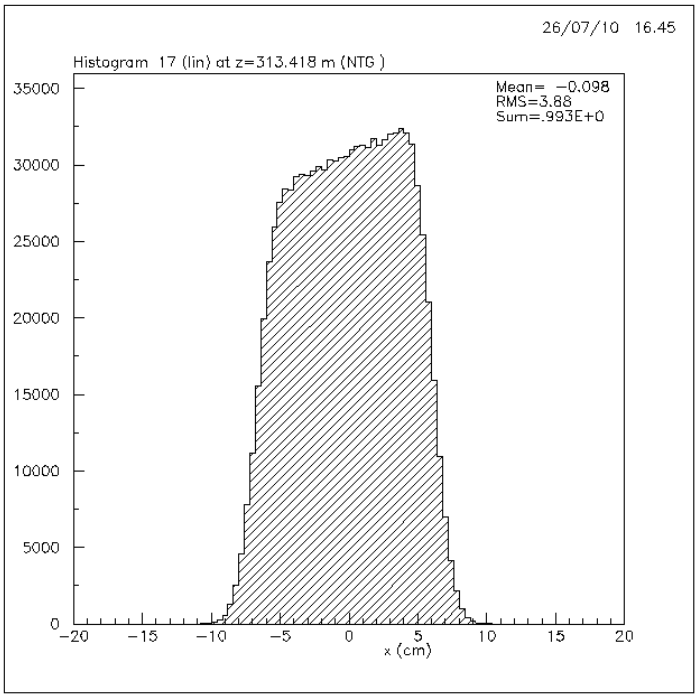

(b)

Figure 7: Horizontal beam profile at mercury target for 2 mm horizontal beam offset at octupole magnet (OCT2). (a) Vertical beam profile, (b) horizontal beam profile.

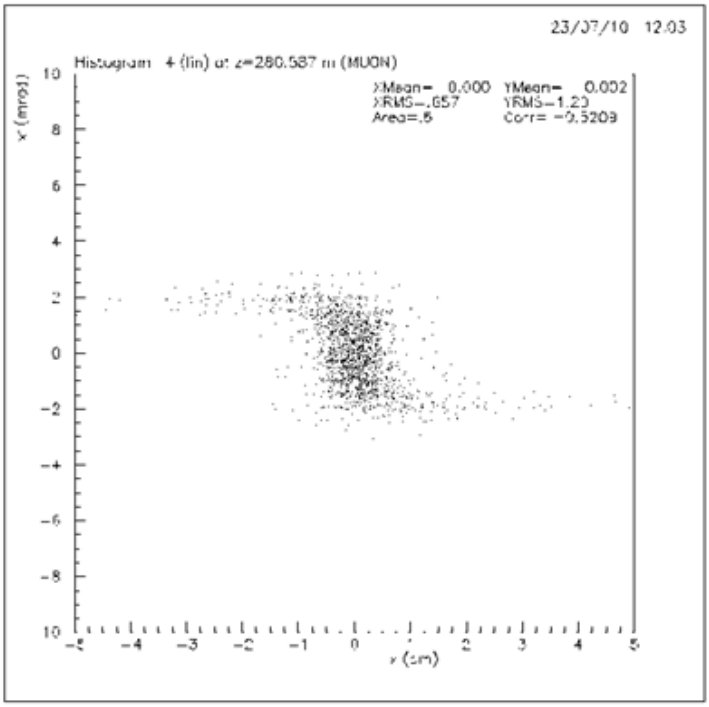

Figure 8: Transverse phase space distribution in horizontal direction for beam injected into muon production target.

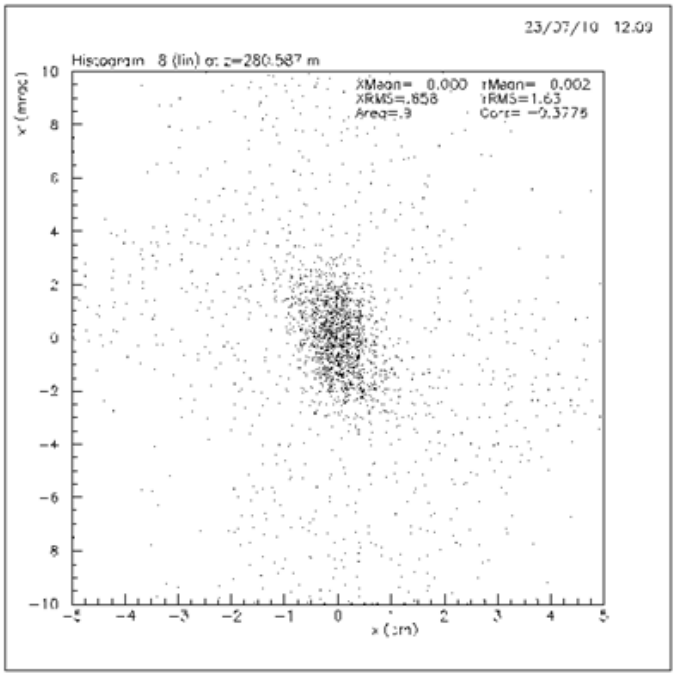

Figure 9: Transverse phase space distribution in horizontal direction for beam scattered from muon production target